



Published in final edited form as:

*Circulation*. 2010 February 2; 121(4): 529–536. doi:10.1161/CIRCULATIONAHA.109.862946.

## Failure of post-natal ductus arteriosus closure in prostaglandin transporter-deficient mice:

### Patent Ductus Arteriosus & Prostaglandin Transporter

Hee-Yoon Chang, Ph.D.<sup>\*</sup>, Joseph Locker, M.D., Ph.D.<sup>§</sup>, Run Lu, M.D.<sup>\*</sup>, and Victor L. Schuster, M.D.<sup>\*,#</sup>

<sup>\*</sup> Department of Medicine, Albert Einstein College of Medicine, Bronx, N.Y. 10461

<sup>§</sup> Department of Pathology, Albert Einstein College of Medicine, Bronx, N.Y. 10461

<sup>#</sup> Department of Physiology and Biophysics, Albert Einstein College of Medicine, Bronx, N.Y. 10461

### Abstract

**Background**—Prostaglandin E<sub>2</sub> (PGE<sub>2</sub>) plays a major role both in maintaining patency of the fetal ductus arteriosus (DA) and in closure of the DA after birth. The rate-limiting step in PGE<sub>2</sub> signal termination is PGE<sub>2</sub> uptake by the transporter PGT.

**Methods and results**—To determine the role of PGT in DA closure, we used a gene-targeting strategy to produce mice in which PGT exon 1 was flanked by loxP sites. Successful targeting was obtained since neither mice hypomorphic at the PGT allele (PGT Neo/Neo) nor global PGT knockout mice (PGT <sup>-/-</sup>) exhibited PGT protein expression; moreover, embryonic fibroblasts isolated from targeted mice failed to exhibit carrier-mediated PGE<sub>2</sub> uptake. Although born in a normal Mendelian ratio, no PGT <sup>-/-</sup> mice survived past post-natal day 1, and no PGT Neo/Neo mice survived past post-natal day 2. Necropsy revealed patent DA with normal intimal thickening but with dilated cardiac chambers. Both PGT Neo/Neo and PGT <sup>-/-</sup> mice could be rescued through the post-natal period by giving the mother indomethacin before birth. Rescued mice grew normally and had no abnormalities by gross and microscopic post-mortem analysis. In accord with PGT's known role in metabolizing PGE<sub>2</sub>, rescued adult PGT <sup>-/-</sup> mice had lower plasma PGE<sub>2</sub> metabolite levels, and higher urinary PGE<sub>2</sub> excretion rates, than wild type mice.

**Conclusions**—PGT plays a critical role in closure of the DA after birth by ensuring a reduction in local and/or circulating PGE<sub>2</sub> concentrations.

---

Correspondence: Victor L. Schuster, M.D., Department of Medicine, Albert Einstein College of Medicine, Belfer Building, Room 1008, Bronx, N.Y. 10461, Phone: (718) 430-8560; FAX (718) 430-8659, schuster@aecom.yu.edu.

Prostaglandins are small signaling molecules that control multiple bodily functions. Many people manipulate their prostaglandin levels without knowing it, because non-steroidal anti-inflammatory drugs, such as aspirin, act by blocking prostaglandin synthesis. Amongst their actions, prostaglandins help to keep open a blood vessel in the fetus called the ductus arteriosus, and to close the ductus appropriately after birth. The present study focuses on the mechanism by which prostaglandin signaling is shut off. Previous experiments, using cells grown in glass dishes, had demonstrated that a carrier protein called PGT transports prostaglandins from the blood into the cell interior, where an enzyme inactivates them. The prediction from these studies would be that inactivating or blocking PGT in an experimental animal or human being would cause prostaglandin levels to rise, resulting in abnormal prostaglandin signaling from one cell to another. Here the authors used genetic engineering methods to inactivate all PGT carriers in mice. They found that mice lacking PGT from conception failed to close their ductus arteriosus normally at birth, resulting in their death on or about the first day of life. The results have implications for humans, since failure to close the ductus arteriosus after birth is a common congenital disorder.

### Disclosures

None.

## Keywords

prostaglandins; ductus arteriosus; patent; heart failure; genes

## Introduction

Prostaglandin E<sub>2</sub> (PGE<sub>2</sub>) modulates many physiological functions<sup>1</sup>. In particular, PGE<sub>2</sub> maintains patency of the ductus arteriosus (DA) *in utero*<sup>2, 3</sup>. Disruption of any of several steps in PGE<sub>2</sub> signaling or signal termination results in patent DA (PDA) after birth<sup>2, 4–8</sup>.

Our laboratory identified the PG transporter PGT<sup>9</sup>, which we have proposed to be responsible for the PGE<sub>2</sub> uptake step in signal termination<sup>10, 11</sup>. PGT's broad tissue expression, high affinity for PGE<sub>2</sub>, and strong expression in the lung suggest that it mediates the well-described single pass metabolic pulmonary clearance<sup>12, 13</sup>. Recently, we co-expressed PGT and 15-hydroxy prostaglandin dehydrogenase (PGDH), showing that the membrane uptake step is rate-limiting for overall PGE<sub>2</sub> catabolism<sup>11</sup>.

To test the hypothesis that PGT plays a central role in controlling pericellular PGE<sub>2</sub> concentrations<sup>10</sup>, and thus signaling via PGE<sub>2</sub> (EP) receptors, we deleted mouse PGT *in vivo* using gene targeting methods. Our results indicate that targeted deletion of mouse PGT deletion leads to a persistent ductus arteriosus which, in turn, results in neonatal mortality.

## Methods

### Construction of targeting vector and conditional PGT knockout mice

A 2.2 kb region containing PGT exon 1 (E1) was targeted for deletion (Figure 1). A 13 kb mouse genomic DNA fragment containing PGT exon 1 was subcloned from a mouse 129 Sv/Ev lambda genomic library. The neomycin resistance cassette (Neo), flanked by both FRT and loxP sites, was inserted 490 bp downstream of exon 1. A third loxP site was inserted 1650 bp upstream of exon 1. The targeting vector was linearized with *Not1* and transfected by electroporation of iTL1 (129Sv/Ev) ES cells. After selection in G418, surviving colonies were expanded, and PCR analysis was performed to identify recombinant clones. The correctly targeted ES cell lines were microinjected into C57Bl/6J blastocysts. Chimeric mice were generated and gave germline transmission of conditional PGT knockout mice, i.e. tri-lox conditional alleles present on a mixed 129Sv and C57Bl/6J genetic background<sup>14</sup>.

### Breeding of the mice and PCR genotyping

Potential founder animals were screened by PCR and further confirmed by Southern blotting (Figure 1). Mouse tail DNA was purified (Qiagen, Valencia, CA) and amplified 35–40 cycles. F0 heterozygous tri-lox conditional alleles (WT/Neo: Figure 1a, line 1 and 2) were detected by PCR using two different primer pairs (pairs 1 and 2 in Table 1S, Supplemental Data). The wild type allele was detected either by primer pair 3 (Figure 1a, line 1: AA', product 2.8 kb) or by primer pair 4 (Figure 1a, line 1: BB', product 1.0 kb). The product from primer pair 3 in Neo/Neo mice was > 5 kb and was not amplified in these conditions.

The Neo gene was then excised by crossing F0 (WT/Neo) with a Rosa 26 FLPe transgenic mouse (129S4/SvJaeSor*Gt(ROSA)26Sor<sup>tm1(FLP1)Dym</sup>/J*, Jackson Laboratories, stock number 003946)<sup>15</sup>, leaving two loxP sites at the targeted locus (Figure 1a, line 3: loxP). The resulting WT/loxP heterozygous (F1) mice were intercrossed to generate homozygous loxP/loxP mice (F2). The loxP allele was detected by PCR using primer pair 5, which flanks the (5'-most) 3<sup>rd</sup> loxP site.

Exon 1 was subsequently excised by crossing loxP/loxP mice with an EIIa Cre transgenic mouse<sup>16</sup> (B6.FVB-Tg (EIIa-cre) C5379Lmgd/J; Jackson Laboratories stock number: 003724) to generate the F3 PGT exon 1 null allele mice (Figure 1a, line 4). These mice were intercrossed to generate WT/WT (PGT+/+), WT/Null (heterozygotes, i.e. PGT+/-), and Null/Null (PGT-/-). PCR results are shown in Figure 1b. The wild type allele was detected as a 2.8 kb fragment, whereas the null allele was detected at 0.6 kb, i.e. after excision of 2.2 kb of exon 1. Since the 2.8 kb fragment was barely detectable in heterozygotes (+/-, Figure 1b middle lane), another primer set flanking exon 1 was designed, which resulted in a 1.0 kb fragment (Figure 1b, bottom panel).

### Southern blot analysis

Genomic DNA (10 µg) from the liver of PGT +/+, +/-, and -/- mice was digested with *HpaI* and used for Southern blot analysis for the PGT alleles (Figure 1c) following standard methods. Hybridization was performed using a 5' external probe (shown as "P" in Figure 1a, line 1), which had been amplified from C57Bl/6J genomic DNA (forward primer 5'-GGGGAAGTATCTGAAGAGGTAAGTCAAG-3'; reverse primer, 5'-GGCAAACATGGCAAATGCTG-3'). This probe recognized a 9.8 kb fragment in wild type mice and a 7.9 kb fragment in null allele mice.

### Generation of PGT -/- mouse embryonic fibroblasts (MEFs) and determination of <sup>3</sup>H-PGE<sub>2</sub> uptake by PGT

We crossed indomethacin-rescued PGT-/- females with PGT +/- males, or intercrossed PGT +/- mice, and euthanized the pregnant females. Embryos at day E14.5 were dissected away from the uterus and decidua. The head was removed for PCR analysis, and the abdomino-thoracic contents and blood clots were removed. The remaining tissue was minced, trypsinized at 37 °C for 15 min, and triturated vigorously. Cell suspensions were washed, plated, and fed with DMEM supplemented with 10% fetal bovine serum. After overnight incubation, floating cells and debris were removed, and fresh medium was added. The resulting MEF cultures were passaged once every 2–3 days.

<sup>3</sup>H-PGE<sub>2</sub> uptake was determined in PGT-/- MEFs using previously described methods<sup>9</sup> in the presence or absence of additional 10 µM unlabeled PGE<sub>2</sub> for 10 min. The PGT-mediated uptake was calculated by subtracting the diffusional uptakes, i.e. uptakes from samples containing 10 µM unlabeled PGE<sub>2</sub>.

### Hematoxylin & Eosin (H&E) stain of DA, and immunohistochemical assessment of PGT expression in neonatal mouse lung and DA

PGT Neo/Neo, PGT+/+, and PGT-/- mice at post-natal day 1 and 2 were examined for morphological abnormalities. After a normal vaginal birth, animals that had died a natural death, or animals that were sacrificed at 11 hours, were placed in 10% neutral buffered formalin overnight and processed for paraffin embedding. Five µm serial transverse sections were cut and mounted on microscope slides. One out of every five sections was stained with H&E. Deparaffinized torso sections were also examined for elastin using Verhoeff's Elastic Stain, which was visualized with 2% ferric chloride followed by 5% sodium thiosulfate, and counterstained with van Gieson solution.

Sections of neonatal mouse lung and ductus arteriosus, and of adult kidney, were subjected to immunohistochemical analysis using standard methods, as previously described<sup>10, 17</sup> using rabbit anti-mouse PGT antibody overnight at 4°C (1:1000 dilution for lung, 1:500 for adult kidney, and 1:400 dilution for ductus). For negative controls, the primary antibody was omitted.

## Plasma PGE<sub>2</sub> metabolite (PGEM) and urinary PGE<sub>2</sub> excretion in wild type and adult rescued PGT<sup>-/-</sup> mice

We collected blood via cardiac puncture from 5–7 month old PGT<sup>-/-</sup> (n = 5) and age-matched PGT<sup>+/+</sup> (n = 6) mice into EDTA and indomethacin (10 μM final concentration). Plasma was stored at -80 C until assay. In separate experiments, using metabolic cages we collected urine from PGT<sup>+/+</sup> (n = 5) and PGT<sup>-/-</sup> (n = 4) mice at 3 to 5 months of age and determined daily urinary PGE<sub>2</sub> excretion. All analyses were done using the PGE<sub>2</sub> monoclonal EIA kit (Cat.# 514010) and PGEM kit (Cat. # 514531) from Cayman Chemical.

### Quantitative Real-Time PCR

Kidneys, hearts, and lungs of adult mice (PGT<sup>-/-</sup>, n = 5; PGT<sup>+/+</sup>, n = 6), and E19 fetus bodies (PGT<sup>-/-</sup>, n = 2; PGT<sup>+/+</sup>, n = 4), were frozen and homogenized with a liquid nitrogen-cooled mortar and pestle, after which RNA was isolated using the RNeasy Mini Kit (Qiagen). For real-time PCR, the QuantiTect™ SYBR®Green RT-PCR kit (Qiagen, 27220 Turnberry Lane Valencia, CA) and 120 ng total RNA were used in the PCR reactions as follows. 1. One cycle of 50°C for 30 minutes and one cycle of 95°C for 16 minutes; 2) forty cycles of 95°C for 15 seconds, 55~58°C for 30 seconds, and 72°C for 30 seconds; and 3) one cycle of 95°C for 15 seconds, 60°C for 15 seconds, and 95°C for 15 seconds. The relative delta delta Ct value was used in the resulting calculation. Some primers were purchased from Qiagen (GeneGlobe products): mGAPDH (QT 01658692), mPGT (QT00140567), mCox-1 (QT00155330), mCox-2 (QT00165347), and mEP<sub>2</sub> (QT00115276). Primers for mEP<sub>4</sub> were custom made by Invitrogen™ (forward primer ATGGTCATCTTACTCATCGCC, reverse primer GCAAATCTGGGTTTCTGCTG). The data were normalized to mGAPDH mRNA; the expression of each gene of interest (PGT, COX1, COX2, EP<sub>2</sub>, and EP<sub>4</sub>) from each mouse was then normalized to the level of expression in mouse #6 (one of the adult WT mice) or 1Q-3 (one of the WT embryos).

### Rescue of PGT Neo/Neo and PGT<sup>-/-</sup> mice by indomethacin

Pregnant female mice bearing PGT Neo/Neo or PGT<sup>-/-</sup> fetuses were administered indomethacin (Indocin 1mg, Merck and CO, INC, PA, USA) orally in a single dose at 3 mg/kg BW 3–9 hours prior to parturition.

### Statistic Analysis

Data are expressed as the mean ± SEM. Comparisons were made using the t-test or the Wilcoxon nonparametric test. Differences were considered significant when  $P < 0.05$ .

### Statement of responsibility

The authors had full access to the data and take responsibility for its integrity. All authors have read and agree to the manuscript as written.

## Results

### PGT targeted mice lack PGT protein expression in the lung and PGE<sub>2</sub> uptake in embryonic fibroblasts

We confirmed the lack of PGT protein expression in PGT Neo/Neo (Fig 2) and PGT<sup>-/-</sup> mice (data not shown) by immunohistochemistry on neonatal lung, which is the tissue with the highest PGT expression in the normal animal<sup>9, 18, 19</sup>. PGT is expressed in the type II alveolar cells lining the alveolar spaces in the PGT<sup>+/+</sup> mice (Figure 2a and Supplemental Data Figure 1S<sup>20</sup>); these cells also express PGDH<sup>21</sup>. In contrast, the lungs of PGT Neo/Neo mice had no discernable PGT protein expression.

In separate experiments (Figure 2b), MEFs from PGT  $+/+$  mice exhibited carrier-mediated  $^3\text{H-PGE}_2$  uptake as evidenced by a 30% augmented uptake when the competitor for PGT (unlabeled  $\text{PGE}_2$ ) was absent. In contrast, MEFs from PGT  $-/-$  mice failed to demonstrate carrier-mediated  $^3\text{H-PGE}_2$  uptake.

Together, these results demonstrate successful knockout of PGT expression in the targeted animals.

### Normal Mendelian birth ratios PGT targeted mice

We examined whether intercrossing WT/Neo heterozygotes resulted in a normal Mendelian ratio of F0 mice. Genotypes were determined in newborn pups from 79 pups (8 litters); the genotyping results showed 21 PGT  $+/+$  mice (27%), 39 PGT  $+/\text{Neo}$  mice (49%), and 19 Neo/Neo mice (24%). In separate experiments, we genotyped 63 newborn pups (6 litters) from PGT  $+/-$  x PGT  $+/-$  crosses. The genotyping results were 18 PGT  $+/+$  (29%), 33 PGT  $+/-$  (52%), and 12 PGT  $-/-$  (19%). Thus, both mice in which the Neo cassette is retained in PGT intron 1, and mice completely lacking PGT exon 1, were born in a normal Mendelian ratio.

### Patent ductus arteriosus in PGT Neo/Neo and PGT $-/-$ mice

Despite normal Mendelian birth ratios in newborn pups, no PGT  $-/-$  mice survived past post-natal day 1, and no PGT Neo/Neo mice survived past post-natal day 2. Cross sections of torsos of PGT  $+/+$  mice ( $n = 3$ ) at post-natal day 1 showed normal closure of the DA (Figure 3a, arrow). On high power examination, intimal thickening in the form of proliferation of luminal endothelium and migration of medial smooth muscle cells was apparent in the DA of these mice (Figure 3d) <sup>22</sup>.

In contrast, PGT Neo/Neo mice ( $n = 5$ ) at post-natal day-1 or -2 showed patent ductus arteriosus PDA (Figure 3b, arrow; the PDA connects the main pulmonary artery to the descending aorta). Similarly, PGT  $-/-$  mice ( $n = 5$ ) failed to close the DA at postnatal day 1 (Figure 3c, arrow). On high power examination, DAs from both PGT Neo/Neo and PGT  $-/-$  mice showed a single endothelial layer (Figure 3e and 3f, respectively) with an open lumen that was covered by a layer of normal intimal thickening.

Just prior to birth (day E19), the endothelium and underlying intimal layers of the DA of PGT targeted mice were histologically normal (Figure 4), indicating that targeting PGT did not induce intrinsic structural malformations of the DA vasculature.

Microscopic examination of the hearts of PGT Neo/Neo and PGT  $-/-$  mice that had died at post-natal day 1 from PDA revealed dilated cardiac chambers (Figure 5b and 5c, respectively) compared with those of wild type mice (Figure 5a), consistent with left-to-right shunt and volume overload congestive heart failure.

### PGT expression in the ductus arteriosus

We immunolabeled sections of mouse torso using a rabbit polyclonal antiserum directed against mouse PGT. As shown in Figure 6, there was strong labeling in smooth muscle cells of the DA intimal thickening in post-natal day 1 wild type mice (Figure 6a,  $n = 3$ ). In contrast, there was no such PGT labeling in the negative control (data not shown), or in the DA of post-natal day 1 PGT Neo/Neo mice (Figure 6b,  $n = 3$ ).

### Rescue of both PGT Neo/Neo and PGT $-/-$ mice by indomethacin

To test the hypothesis that high levels of  $\text{PGE}_2$  in the post-partum period lead to PDA in PGT targeted mice, we administered the nonselective cyclooxygenase inhibitor indomethacin to pregnant mice several hours before birth (i.e. at fetal day E19) to lower  $\text{PGE}_2$  concentrations

in the newborn pups. All pups subjected to maternal indomethacin rescue, including PGT  $-/-$ , survived the neonatal period. Histological examination of a rescued 2 week-old PGT Neo/Neo mouse demonstrated a normally closed DA (converted into the ligamentum arteriosum<sup>22</sup>) (data not shown).

### **Blood PGE<sub>2</sub> metabolite (PGEM) concentration, and urinary PGE<sub>2</sub> excretion, in indomethacin-rescued PGT $-/-$ mice compared to PGT $+/+$ mice**

To test the hypothesis that PGE<sub>2</sub> is not metabolized at a normal rate in PGT  $-/-$  mice, we measured plasma PGEM concentrations in 5–7 month old PGT  $+/+$  mice (n = 6) compared to those of age-matched PGT  $-/-$  mice that were products of maternal indomethacin rescue (n = 5). Plasma PGEM concentrations were  $2644 \pm 751$  pg/mL in the PGT  $+/+$  type mice and  $856 \pm 295$  pg/mL in the adult PGT  $-/-$  mice (p = 0.027 by one-tailed t-test; p = 0.022 by Wilcoxon two-sample test). These results are consistent with a failure to metabolize PGE<sub>2</sub> in the PGT  $-/-$  mice.

In separate experiments, we determined 24-hour urinary PGE<sub>2</sub> excretion in adult mice that were the product of maternal indomethacin rescue. Urinary PGE<sub>2</sub> levels were significantly higher in PGT  $-/-$  mice compared to PGT  $+/+$  mice ( $3073 \pm 756$  pg/day, n = 4, versus  $1497 \pm 187$  pg/day, n = 5, respectively, p < 0.05 by unpaired t-test). These results are also consistent with a failure of PGT null mice to metabolize PGE<sub>2</sub>.

### **Modulation of the PGE<sub>2</sub> signaling pathway in PGT $-/-$ mice**

PGT  $-/-$  mice grew normally and were histologically normal at necropsy (n = 5 adult mice, data not shown). We measured mRNA levels for PGT, COX-1, COX-2, and the PGE<sub>2</sub> receptors EP2 and EP4 in mouse embryos just prior to birth, and also in mouse kidney, lung, and heart from adult mice. Supplemental data, Table 2S, shows that, in PGT  $-/-$  mice, PGT mRNA levels were significantly decreased to background noise values in whole embryos and in all three tissues from rescued adult animals. In the rescued adult PGT  $-/-$  mice compared to PGT  $+/+$  mice, lung tissue revealed a statistically significant decrease in COX-1 mRNA; heart revealed a statistically significant increase in EP<sub>2</sub> mRNA; and kidney revealed a statistically significant increase in EP<sub>4</sub> mRNA.

Separately, we carried out immunocytochemical labeling of COX-1 and COX-2 in the lungs and kidneys of PGT  $-/-$  and PGT  $+/+$  mice. These studies revealed no discernable difference in COX-1 or COX-2 expression (Supplemental Data, Figure 2S).

## **Discussion**

These studies reveal that mice hypomorphic (“Neo/Neo”) or null (“PGT  $-/-$ ”) at the PGT locus fail to close the DA during postnatal days 1–2, resulting in PDA. The latter causes cardiac biventricular chamber dilatation, consistent with the presence of a postnatal left-to-right shunt. Morphologically, the endothelium and internal elastic lamina of the DA of PGT Neo/Neo and PGT  $-/-$  embryos just prior to birth appeared normal. PGT targeted mice established a normal intimal thickening, but failed to constrict the DA after birth. Both PGT Neo/Neo and PGT  $-/-$  mice could be rescued through the post-natal period by administering indomethacin to the mother several hours before birth. Adult rescued PGT null mice had significantly lower plasma PGE<sub>2</sub> metabolite levels, and significantly higher urinary PGE<sub>2</sub> excretion rates, than wild type mice, consistent with their failure to metabolize systemic PGE<sub>2</sub>.

The DA connects the fetal pulmonary artery and descending aorta. Although the DA closes immediately after birth, it remains open in some infants, a condition known as PDA<sup>23</sup>. Nonselective COX inhibitors, such as indomethacin, have long been used to successfully treat

PDA in patients<sup>24</sup>, results that are consistent with a large body of literature pointing to a central role of PGE<sub>2</sub> in maintaining DA patency<sup>8, 23, 25–27</sup>.

A current model postulates two separate roles for PGE<sub>2</sub> in DA closure. In late fetal life and continuing after birth, PGE<sub>2</sub> controls formation of the intimal cushion (or thickening) via EP<sub>4</sub> receptors<sup>3, 4, 7, 22, 28, 29</sup>. Post-natally, loss of the placenta as a source of PGE<sub>2</sub><sup>30</sup>, and PGE<sub>2</sub> metabolism, especially within the pulmonary circulation<sup>12</sup>, result in falling circulating PGE<sub>2</sub> levels. These falling PGE<sub>2</sub> levels induce constriction of the cushion-containing DA<sup>3, 7, 28, 30</sup>. The present data are consistent with this model, i.e. targeting PGT does not interfere with intimal thickening, but rather, persistence of PGE<sub>2</sub> opposes the constrictor mechanism(s) activated by oxygen.

Although PGT transports PGE<sub>2</sub> rapidly and with high affinity<sup>9</sup>, and although our laboratory had previously built a strong circumstantial case that PGT is the major route for reuptake and metabolism of PGE<sub>2</sub><sup>11, 31, 32</sup>, the possibility had remained that either a) prostanoids might not be the “preferred” PGT substrates; or b) other, as yet undiscovered, PG uptake carriers could substitute for PGT. The present results render neither of these two possibilities tenable.

At least in the mouse, disrupting PGE<sub>2</sub> signaling in any of several ways causes PDA. Although genetic disruptions of Cox-1 or Cox-2 alone, or pharmacological disruption of both Cox isoforms, have been reported to produce variable effects on post-natal ductus closure<sup>5, 8, 33–36</sup>, genetic disruption of both Cox isoforms uniformly causes post-natal PDA<sup>5, 8</sup>. Moreover, targeted deletion of the PGE<sub>2</sub>-specific receptor EP<sub>4</sub><sup>4, 7</sup> and targeted deletion of intracellular PGE<sub>2</sub> oxidation, which is catalyzed by PGDH<sup>6</sup> also result in PDA. The present results, i.e. that targeted deletion of PGT also results in PDA, position PGT within the overall PGE<sub>2</sub> signaling pathway (Figure 7).

After birth, systemic PGE<sub>2</sub> concentrations fall<sup>30, 37, 38</sup> with loss of the placenta as a source of PGE<sub>2</sub><sup>30</sup> and metabolism of PGE<sub>2</sub>, especially within the pulmonary circulation<sup>12</sup>. Given that the lung is perfused after birth, that both PGT (present results) and PGDH are strongly expressed in the neonatal lung<sup>39</sup>, and that PGT is rate-limiting for delivering PGE<sub>2</sub> to the cytoplasmic PGDH<sup>11</sup>, PGT would be well positioned to reduce systemic PGE<sub>2</sub> concentrations and initiate closure of the DA after birth.

Due to technical limitations imposed by the extremely small plasma volume of fetal mice, we could not determine whether PGT<sup>-/-</sup> mice have elevated plasma PGE<sub>2</sub> levels *in utero*. Although exogenous PGE<sub>2</sub> added to the post-natal sheep ductus *in vitro* has been shown to regulate genes that regulate calcium availability<sup>36</sup>, we found that whole-embryo mRNA levels for Cox-1 and Cox-2, and for EP<sub>2</sub> and EP<sub>4</sub> receptors, showed no difference between wild type and PGT null mice (Table 2S). On the other hand, indomethacin-rescued adult PGT<sup>-/-</sup> mice demonstrated down-regulation of lung Cox-1 mRNA, and up-regulation of heart EP<sub>2</sub> mRNA and of kidney EP<sub>4</sub> mRNA (Table 2S). This difference raises the possibility that the PGT null fetus is not exposed to abnormally high PGE<sub>2</sub> plasma levels, perhaps because the fetal lungs, although rich in PGT expression (Figure 6), are not perfused *in utero*.

In addition to controlling circulating PGE<sub>2</sub> levels, PGT also operates at a very local level. PGT is often co-expressed in the same cells as COX<sup>17</sup>, and reconstitution experiments have demonstrated PGE<sub>2</sub> synthesis and release, on the one hand, and PGT-mediated reuptake and PGDH-mediated oxidation, on the other, in the same cell<sup>10, 40</sup>. These findings have prompted us to advance a “local release-reuptake model”, analogous to that of neurotransmitter signaling at the synaptic cleft, in which PGT constrains prostaglandins to a highly confined environment, thus facilitating precise autocrine/paracrine signaling<sup>10</sup>. Although there some disagreement as to the extent to which the ductus arteriosus of the term or post-natal mouse expresses one

or both isoforms of cyclooxygenase<sup>5, 8, 34, 36</sup>, the ductus clearly expresses PGE synthase<sup>34</sup> and also exhibits clear labeling for PGT (present results). The vascular endothelium also strongly expresses PGT<sup>41–43</sup>. Taken together, these findings suggest that PGT-mediated PGE<sub>2</sub> uptake occurs, not only systemically in the pulmonary circulation, but also locally in close proximity to the ductus. Further experiments using the isolated mouse ductus obtained from PGT<sup>-/-</sup> versus wild type mice would likely clarify further the influence of PGT of autocrine PGE<sub>2</sub> signaling in this tissue.

In summary, targeted deletion of PGT gene expression in the mouse results in PDA. These results indicate that PGT plays a key role, not only terms of general prostaglandin metabolism, but specifically in terms of modulating PGE<sub>2</sub> signaling.

## Supplementary Material

Refer to Web version on PubMed Central for supplementary material.

## Acknowledgments

We thank the Einstein Mouse Genetics Course for inspiring the gene targeting, and the assistance of the Einstein Cancer Center. We thank Dr. Rani Sellers for phenotyping the PGT global knockout mice.

### Funding Sources

Supported by NIH grants RO1-DK49688 and P50-DK064236.

## References

1. Miller SB. Prostaglandins in health and disease: an overview. *Semin Arthritis Rheum* 2006;36:37–49. [PubMed: 16887467]
2. Schneider DJ, Moore JW. Patent ductus arteriosus. *Circulation* 2006;114:1873–1882. [PubMed: 17060397]
3. Ivey KN, Srivastava D. The paradoxical patent ductus arteriosus. *J Clin Invest* 2006;116:2863–2865. [PubMed: 17080192]
4. Segi E, Sugimoto Y, Yamasaki A, Aze Y, Oida H, Nishimura T, Murata T, Matsuoka T, Ushikubi F, Hirose M, Tanaka T, Yoshida N, Narumiya S, Ichikawa A. Patent ductus arteriosus and neonatal death in prostaglandin receptor EP4-deficient mice. *Biochem Biophys Res Commun* 1998;246:7–12. [PubMed: 9600059]
5. Loftin CD, Trivedi DB, Tiano HF, Clark JA, Lee CA, Epstein JA, Morham SG, Breyer MD, Nguyen M, Hawkins BM, Goulet JL, Smithies O, Koller BH, Langenbach R. Failure of ductus arteriosus closure and remodeling in neonatal mice deficient in cyclooxygenase-1 and cyclooxygenase-2. *Proceedings of the National Academy of Sciences of the United States of America* 2001;98:1059–1064. [PubMed: 11158594]
6. Coggins KG, Latour A, Nguyen MS, Audoly L, Coffman TM, Koller BH. Metabolism of PGE<sub>2</sub> by prostaglandin dehydrogenase is essential for remodeling the ductus arteriosus. *Nat Med* 2002;8:91–92. [PubMed: 11821873]
7. Nguyen M, Camenisch T, Snouwaert JN, Hicks E, Coffman TM, Anderson PA, Malouf NN, Koller BH. The prostaglandin receptor EP4 triggers remodelling of the cardiovascular system at birth. *Nature* 1997;390:78–81. [PubMed: 9363893]
8. Reese J, Paria BC, Brown N, Zhao X, Morrow JD, Dey SK. Coordinated regulation of fetal and maternal prostaglandins directs successful birth and postnatal adaptation in the mouse. *Proc Natl Acad Sci U S A* 2000;97:9759–9764. [PubMed: 10944235]
9. Kanai N, Lu R, Satriano JA, Bao Y, Wolkoff AW, Schuster VL. Identification and characterization of a prostaglandin transporter. *Science* 1995;268:866–869. [PubMed: 7754369]



10. Nomura T, Chang HY, Lu R, Hankin J, Murphy RC, Schuster VL. Prostaglandin signaling in the renal collecting duct: release, reuptake, and oxidation in the same cell. *J Biol Chem* 2005;280:28424–28429. [PubMed: 15855165]
11. Nomura T, Lu R, Pucci ML, Schuster VL. The two-step model of prostaglandin signal termination: in vitro reconstitution with the prostaglandin transporter and prostaglandin 15 dehydrogenase. *Mol Pharmacol* 2004;65:973–978. [PubMed: 15044627]
12. Eling TE, Anderson MW. Studies on the biosynthesis, metabolism and transport of prostaglandins by the lung. *Agents Actions* 1976;6:543–546. [PubMed: 961548]
13. Hawkins HJ, Wilson AG, Anderson MW, Eling TE. Uptake and metabolism of prostaglandins by isolated perfused lung: species comparisons and the role of plasma protein binding. *Prostaglandins* 1977;14:251–259. [PubMed: 897217]
14. Sauer B. Inducible gene targeting in mice using the Cre/lox system. *Methods* 1998;14:381–392. [PubMed: 9608509]
15. Farley FW, Soriano P, Steffen LS, Dymecki SM. Widespread recombinase expression using FLPeR (flipper) mice. *Genesis* 2000;28:106–110. [PubMed: 11105051]
16. Lakso M, Pichel JG, Gorman JR, Sauer B, Okamoto Y, Lee E, Alt FW, Westphal H. Efficient in vivo manipulation of mouse genomic sequences at the zygote stage. *Proc Natl Acad Sci U S A* 1996;93:5860–5865. [PubMed: 8650183]
17. Bao Y, Pucci ML, Chan BS, Lu R, Ito S, Schuster VL. Prostaglandin transporter PGT is expressed in cell types that synthesize and release prostanoids. *Am J Physiol Renal Physiol* 2002;282:F1103–1110. [PubMed: 11997327]
18. Lu R, Kanai N, Bao Y, Schuster VL. Cloning, in vitro expression, and tissue distribution of a human prostaglandin transporter cDNA (hPGT). *J Clin Invest* 1996;98:1142–1149. [PubMed: 8787677]
19. Pucci ML, Bao Y, Chan B, Itoh S, Lu R, Copeland NG, Gilbert DJ, Schuster VL. Cloning of mouse prostaglandin transporter PGT cDNA: species-specific substrate affinities. *Am J Physiol* 1999;277:R734–R741. [PubMed: 10484490]
20. Kalina M, Socher R. Endocytosis in cultured rat alveolar type II cells: effect of lysosomotropic weak bases on the processes. *J Histochem Cytochem* 1991;39:1337–1348. [PubMed: 1658127]
21. Devereux TR, Fouts JR, Eling TE. Metabolism of prostaglandin PGF<sub>2</sub> alpha by freshly isolated alveolar type II cells from lungs of adult male or pregnant rabbits. *Prost Leukotr Med* 1987;27:43–52.
22. Tada T, Kishimoto H. Ultrastructural and histological studies on closure of the mouse ductus arteriosus. *Acta Anat (Basel)* 1990;139:326–334. [PubMed: 2075800]
23. Smith GC. The pharmacology of the ductus arteriosus. *Pharmacol Rev* 1998;50:35–58. [PubMed: 9549757]
24. Heymann MA, Rudolph AM, Silverman NH. Closure of the ductus arteriosus in premature infants by inhibition of prostaglandin synthesis. *N Engl J Med* 1976;295:530–533. [PubMed: 950959]
25. Clyman RI, Mauray F, Roman C, Rudolph AM. PGE<sub>2</sub> is a more potent vasodilator of the lamb ductus arteriosus than is either PGI<sub>2</sub> or 6 keto PGF<sub>1</sub>alpha. *Prostaglandins* 1978;16:259–264. [PubMed: 360304]
26. Clyman RI, Mauray F, Roman C, Rudolph AM, Heymann MA. Circulating prostaglandin E<sub>2</sub> concentrations and patent ductus arteriosus in fetal and neonatal lambs. *J Pediatr* 1980;97:455–461. [PubMed: 6902770]
27. Clyman RI. Ductus arteriosus: current theories of prenatal and postnatal regulation. *Semin Perinatol* 1987;11:64–71. [PubMed: 3551085]
28. Yokoyama U, Minamisawa S, Quan H, Ghatak S, Akaike T, Segi-Nishida E, Iwasaki S, Iwamoto M, Misra S, Tamura K, Hori H, Yokota S, Toole BP, Sugimoto Y, Ishikawa Y. Chronic activation of the prostaglandin receptor EP<sub>4</sub> promotes hyaluronan-mediated neointimal formation in the ductus arteriosus. *J Clin Invest* 2006;116:3026–3034. [PubMed: 17080198]
29. Yokoyama U, Minamisawa S, Quan H, Akaike T, Suzuki S, Jin M, Jiao Q, Watanabe M, Otsu K, Iwasaki S, Nishimaki S, Sato M, Ishikawa Y. PGE<sub>2</sub>-activated Epac promotes neointimal cushion formation of the rat ductus arteriosus by a process distinct from that of PKA. *J Biol Chem* 2008;283:28702–28709. [PubMed: 18697745]

30. Thorburn GD. The placenta, PGE2 and parturition. *Early Hum Dev* 1992;29:63–73. [PubMed: 1327713]
31. Schuster VL. Prostaglandin transport. *Prostaglandins Other Lipid Mediat* 2002;68–69:633–647.
32. Schuster VL. Molecular mechanisms of prostaglandin transport. *Annu Rev Physiol* 1998;60:221–242. [PubMed: 9558462]
33. Loftin CD, Trivedi DB, Langenbach R. Cyclooxygenase-1-selective inhibition prolongs gestation in mice without adverse effects on the ductus arteriosus. *J Clin Invest* 2002;110:549–557. [PubMed: 12189249]
34. Baragatti B, Brizzi F, Ackerley C, Barogi S, Ballou LR, Coceani F. Cyclooxygenase-1 and cyclooxygenase-2 in the mouse ductus arteriosus: individual activity and functional coupling with nitric oxide synthase. *Br J Pharmacol* 2003;139:1505–1515. [PubMed: 12922938]
35. Sodini D, Baragatti B, Barogi S, Laubach VE, Coceani F. Indomethacin promotes nitric oxide function in the ductus arteriosus in the mouse. *Br J Pharmacol* 2008;153:1631–1640. [PubMed: 18297107]
36. Reese J, Waleh N, Poole SD, Brown N, Roman C, Clyman RI. Chronic in utero cyclooxygenase inhibition alters PGE2-regulated ductus arteriosus contractile pathways and prevents postnatal closure. *Pediatr Res* 2009;66:155–161. [PubMed: 19390487]
37. Challis JR, Dille SR, Robinson JS, Thorburn GD. Prostaglandins in the circulation of the fetal lamb. *Prostaglandins* 1976;11:1041–1052. [PubMed: 935521]
38. Mitchell MD, Brunt J, Clover L, Walker DW. Prostaglandins in the umbilical and uterine circulations during late pregnancy in the ewe. *J Reprod Fertil* 1980;58:283–287. [PubMed: 7431261]
39. Sun FF, Armour SB. Prostaglandin 15-hydroxy dehydrogenase and delta13 reductase levels in the lungs of maternal, fetal and neonatal rabbits. *Prostaglandins* 1974;7:327–338. [PubMed: 4370299]
40. Pucci ML, Endo S, Nomura T, Lu R, Khine C, Chan BS, Bao Y, Schuster VL. Coordinate control of prostaglandin E2 synthesis and uptake by hyperosmolarity in renal medullary interstitial cells. *Am J Physiol Renal Physiol* 2006;290:F641–649. [PubMed: 16263809]
41. Topper JN, Cai J, Stavrakis G, Anderson KR, Woolf EA, Sampson BA, Schoen FJ, Falb D, Gimbrone MA Jr. Human prostaglandin transporter gene (hPGT) is regulated by fluid mechanical stimuli in cultured endothelial cells and expressed in vascular endothelium in vivo. *Circulation* 1998;98:2396–2403. [PubMed: 9832484]
42. Dekker RJ, Boon RA, Rondaij MG, Kragt A, Volger OL, Elderkamp YW, Meijers JC, Voorberg J, Pannekoek H, Horrevoets AJ. KLF2 provokes a gene expression pattern that establishes functional quiescent differentiation of the endothelium. *Blood* 2006;107:4354–4363. [PubMed: 16455954]
43. McCormick SM, Eskin SG, McIntire LV, Teng CL, Lu CM, Russell CG, Chittur KK. Dna microarray reveals changes in gene expression of shear stressed human umbilical vein endothelial cells. *Proceedings of the National Academy of Sciences of the United States of America* 2001;98:8955–8960. [PubMed: 11481467]

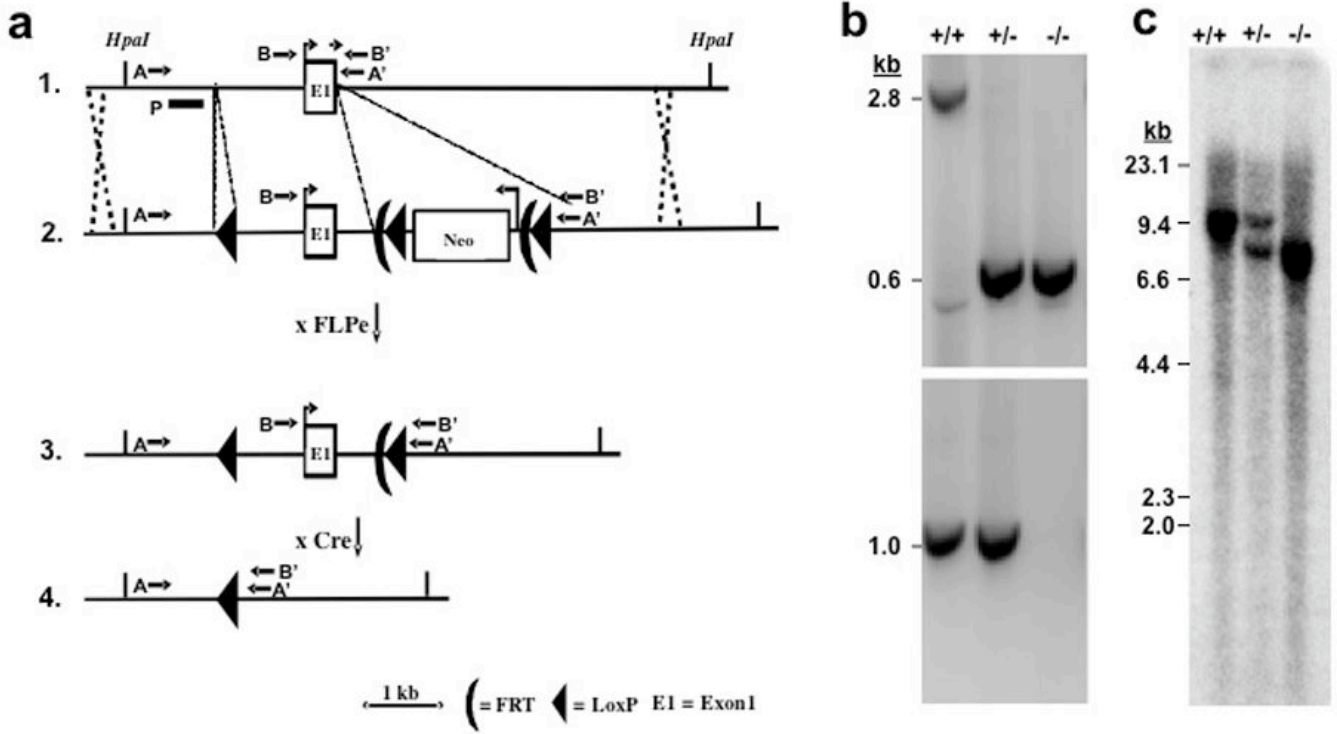


**Figure 1. Targeting strategy for knocking out the mouse PGT gene**

(a) Strategy used for PGT gene targeting. Top line: endogenous locus; 2nd line: targeting vector; 3rd line: targeted locus after excision of Neo gene cassette with FLPe; Bottom line: targeted locus after excision of Exon 1 at LoxP sites with Cre recombinase. A targeting vector containing a 13 kb mouse genomic DNA segment was constructed with 3 LoxP insertions, two of them flanking a Neo gene insertion, which also includes two FLPe recombinase sites. The locations of PCR primers (AA' or BB') are shown by arrows. P signifies the hybridization probe for Southern blots.

(b) Genotyping of wild type (+/+), heterozygote (+/-), and global KO mice (-/-). PCR products from the intact PGT Exon 1 gene and from the gene lacking Exon 1 generated 2.8 kb and 0.6 kb fragment, respectively (Primers AA'). Because of competition in the PCR reaction, both products could not be visualized in DNA from heterozygotes. Therefore, a second PCR reaction (BB': 1.0 kb) was used to demonstrate the wild type allele (bottom gel). Global KO mice show only 0.6 kb.

(c) A restriction enzyme *HpaI* as used for Southern blot hybridization. A 9.8 kb band in the wild type allele was replaced by an 7.9 kb band in the targeted allele.

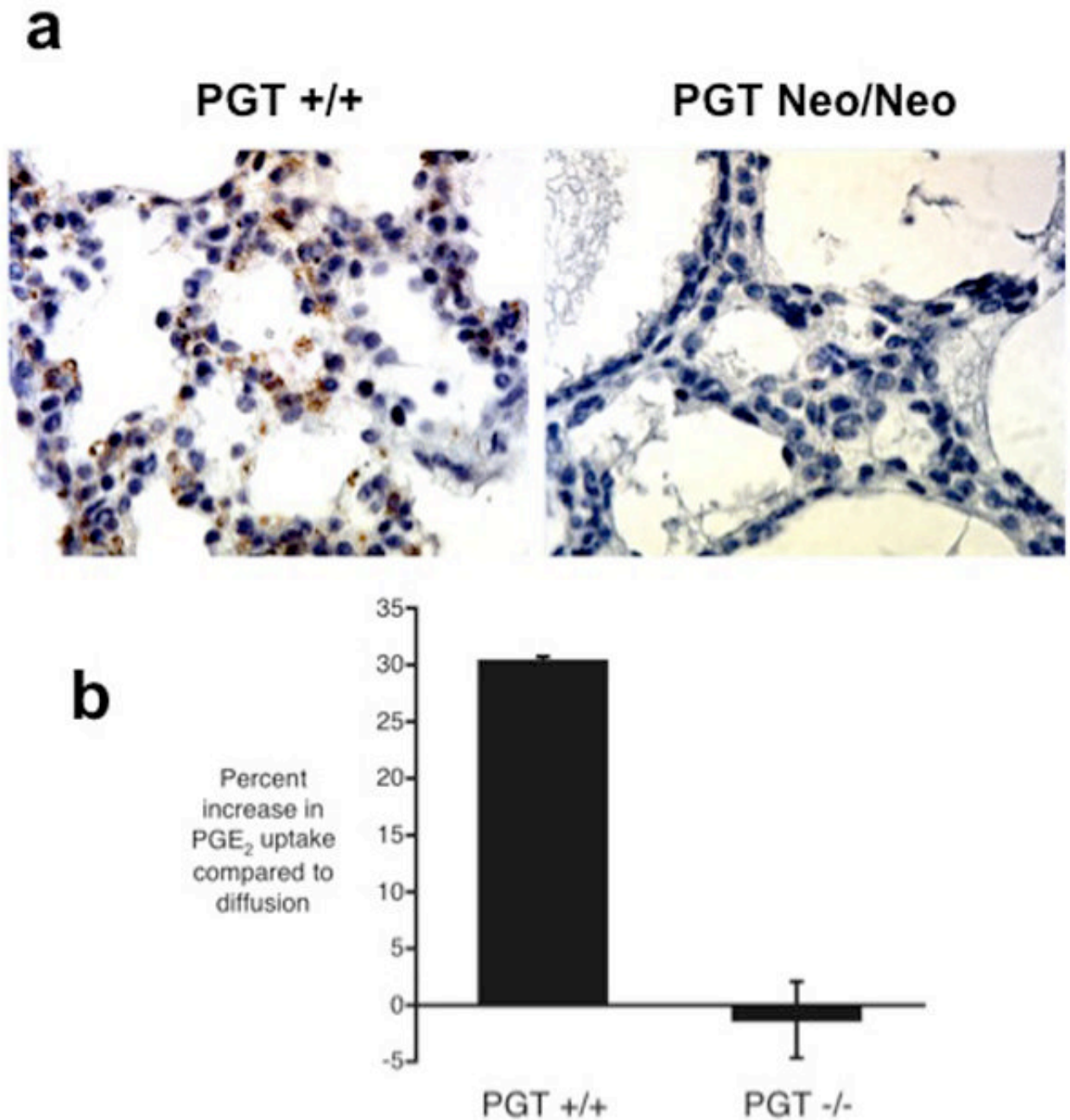


**Figure 2. Validation of PGT targeting by loss of protein expression and transport function**

**(a)** Lung tissue from PGT Neo/Neo mice shows absence of PGT protein, whereas PGT +/+ mice express PGT (brown reaction product) in type II cells (see Supplemental Data Figure 1S for birefringence of granules of these cells in our PGT +/+ mice).

**(b)** PGE<sub>2</sub> uptake by mouse embryonic fibroblasts (MEFs) derived from PGT wild type (+/+) versus PGT null (-/-) mice. <sup>3</sup>H-PGE<sub>2</sub> uptake was determined alone (this represents PGT-mediated uptake plus simple diffusion) and also in the presence of excess unlabeled PGE<sub>2</sub> (this blocks PGT-mediated tracer uptake and reveals uptake due to simple diffusion alone). For each set of paired uptake data, we calculated the percent increase in PGE<sub>2</sub> uptake attributable to PGT:  $(\text{uptake}_{\text{tracer}}) \div (\text{uptake}_{\text{tracer} + \text{unlabeled}}) \times 100$ . MEFs from PGT +/+ mice (n = 7) had a

PGT-mediated change in uptake of  $+30.3\% \pm 8.38\%$  ( $n = 7$ ), whereas MEFs derived from PGT  $-/-$  animals had a PGT-mediated change in uptake of  $-1.29\% \pm 3.38\%$  ( $n = 7$ ). The difference was highly statistically significant ( $p = 0.008$  by unpaired t-test;  $p = 0.007$  by Wilcoxon two-sample test).

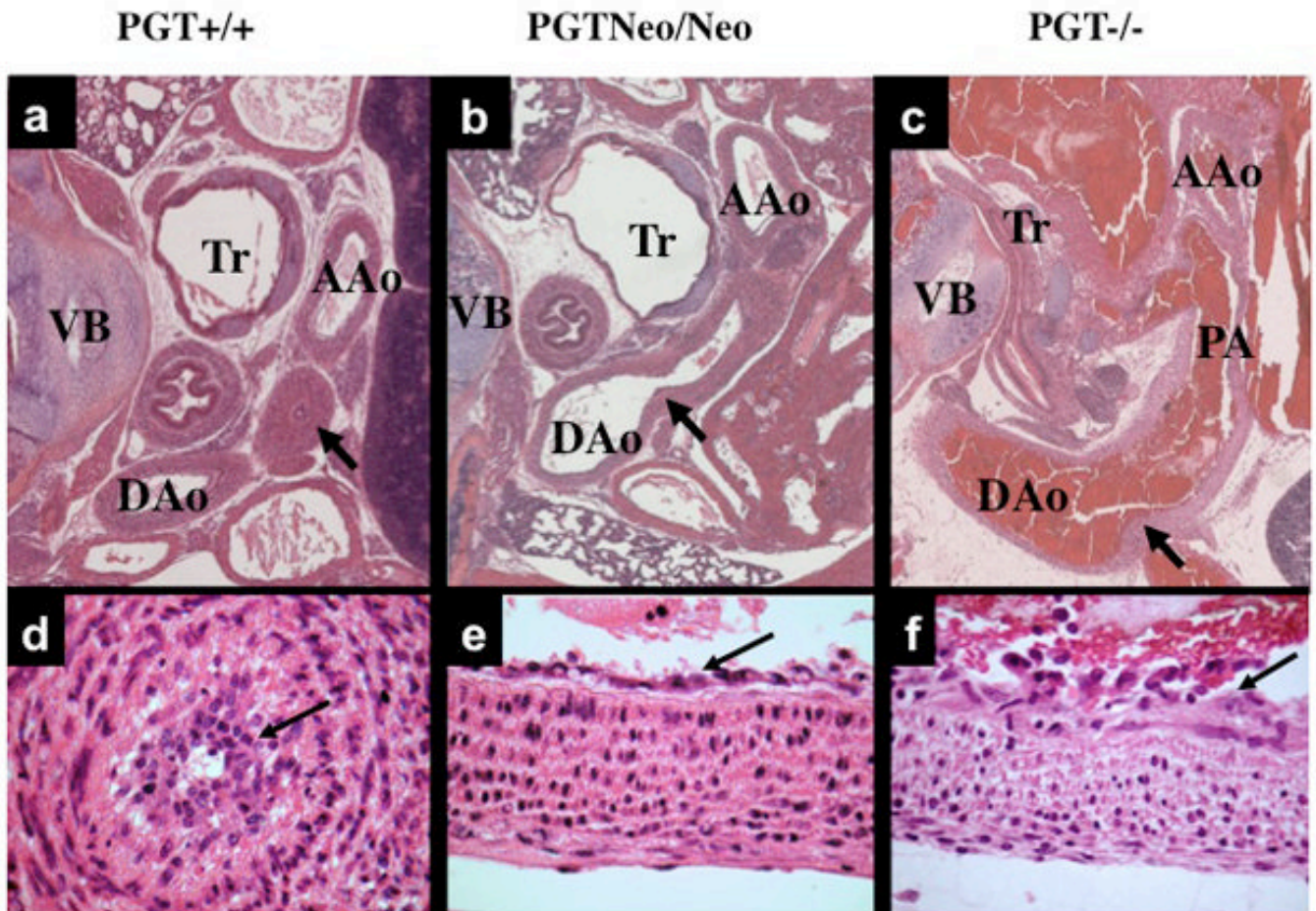


**Figure 3. Patent DA in PGT Neo/Neo and PGT -/- mice**  
H&E stain of paraffin-embedded sections.

(a) and (d). Low- and high-power view, respectively, of a cross-section from the torso of a PGT +/+ (wild type) mouse (representative, n = 3) eleven hours after birth. The DA has closed normally (a, arrow), and there is a normal intimal thickening (d, arrow) consisting of a loose network of cells filling and obliterating the constricted lumen. Tr, trachea; VB, vertebra; AAo, ascending aorta; DAo, descending aorta.

(b) and (e). Torso of PGT Neo/Neo mouse (representative, n = 5) dying on post-natal day 2 shows PDA. An arrow marks the connection between the DAo and DA. High power view (e) reveals normal intimal thickening (arrow).

(c) and (f). Torso of PGT -/- mouse (representative, n = 5) similarly shows patent DA. The pulmonary artery (PA) has dilated with reversed blood flow, and blood also fills the DAo and PA. High power (f) view reveals normal intimal thickening (arrow).

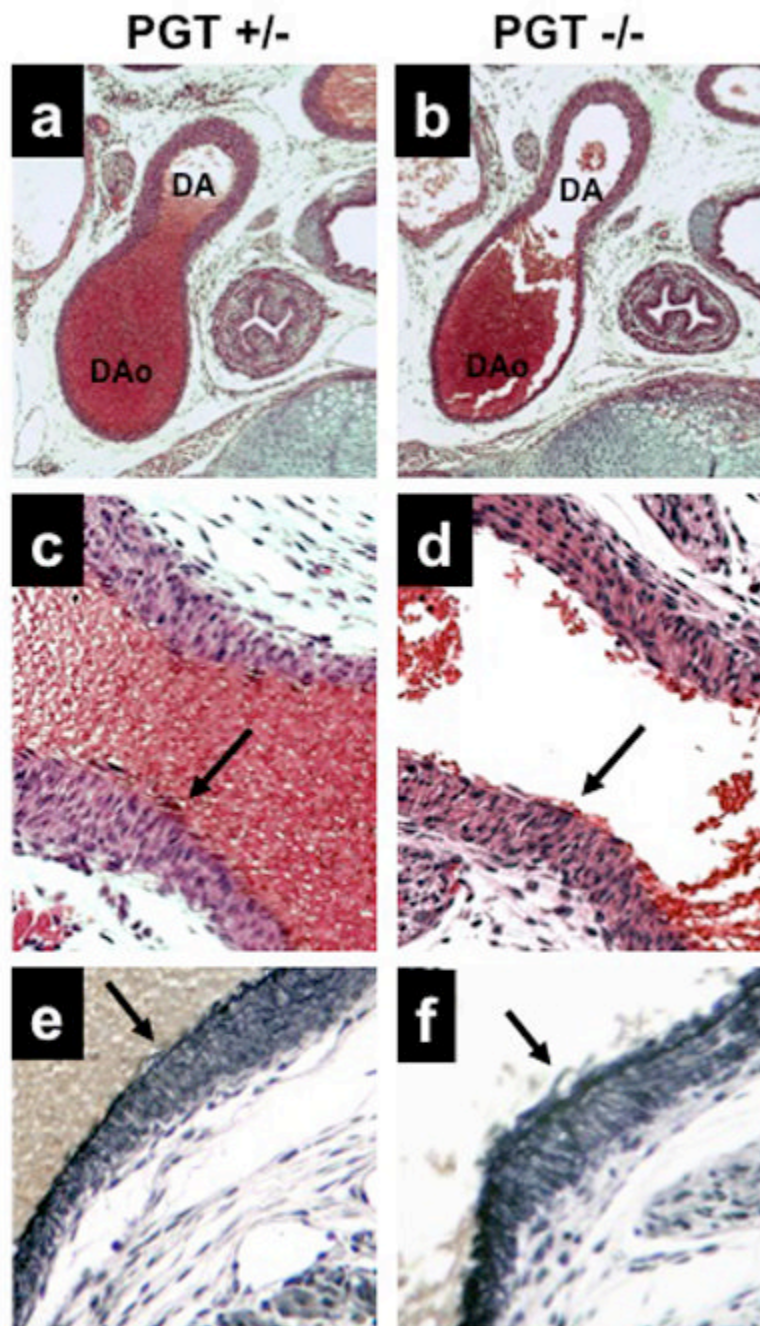


**Figure 4. Endothelium and internal elastic lamina of the DA at embryonic day E19 appear normal in PGT targeted mice**

(a, c, e) PGT heterozygote (+/-) examined at embryonic day E19 shows the expected patent DA in continuity with the descending aorta (DAo) (a) with a normal-appearing endothelium in H&E staining (arrow, c) and normal elastin staining of the internal elastic lamina (arrow, e).

(b, d, f) PGT null mouse (PGT -/-) shows the same pattern as the PGT +/- mouse.

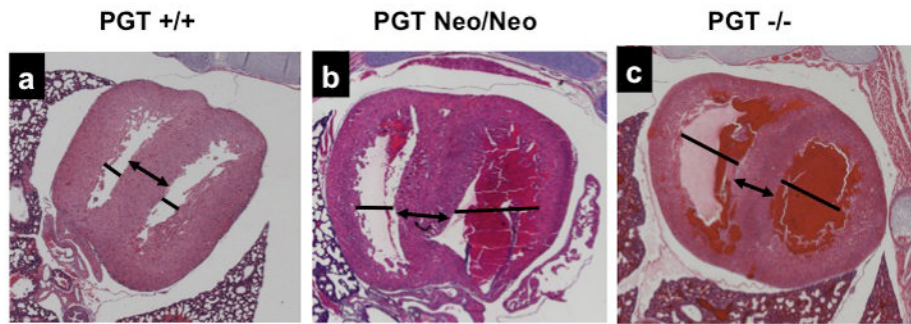


**Figure 5. Hearts of PGT targeted mice show chamber dilatation with normal interventricular septum thickness**

**(a)** Wild type mice (n = 3) have normal dimensions of the cardiac chambers (solid line). The interventricular septum, an indicator of intrinsic myocardial muscle development, is also normal (arrow).

**(b)** PGT Neo/Neo mouse (n = 3) shows dilated right and left ventricular chambers (lines), but the interventricular septum, an indicator of intrinsic heart muscle development, is normal (arrow).

**(c)** PGT  $-/-$  mouse (n = 3) shows finding similar to (b).



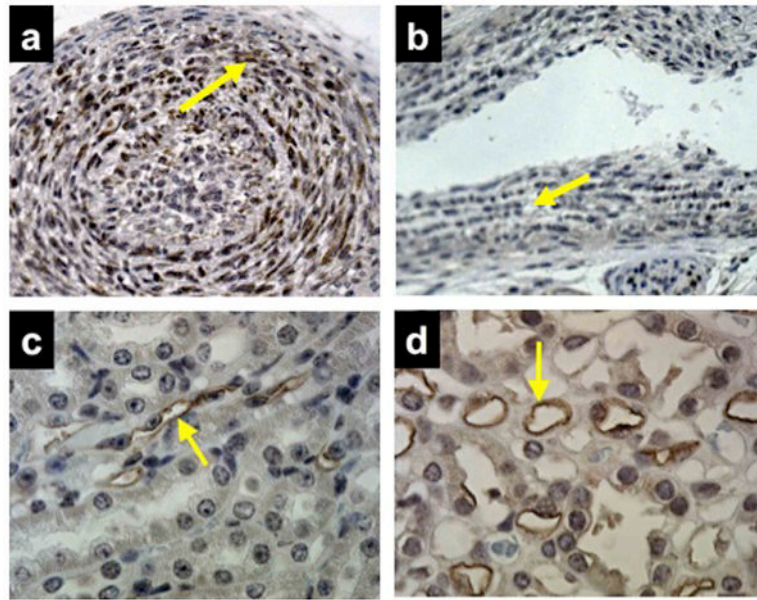


**Figure 6. Immunolabeling for PGT shows strong expression in the normal DA compared to the kidney**

**(a)** DA of wild type mouse (n = 3) on post-natal day 1 showing strong labeling for PGT in smooth muscle cells of the myointimal thickening (brown reaction product, arrow).

**(b)** DA of PGT Neo/Neo mouse (n = 3) on post-natal day 1 with negative PGT labeling (arrow).

**(c and d)** Labeling of mouse renal cortical collecting duct (c, arrow) and mouse renal papillary vasa recta endothelium (d, arrow) as positive controls (n = 10).

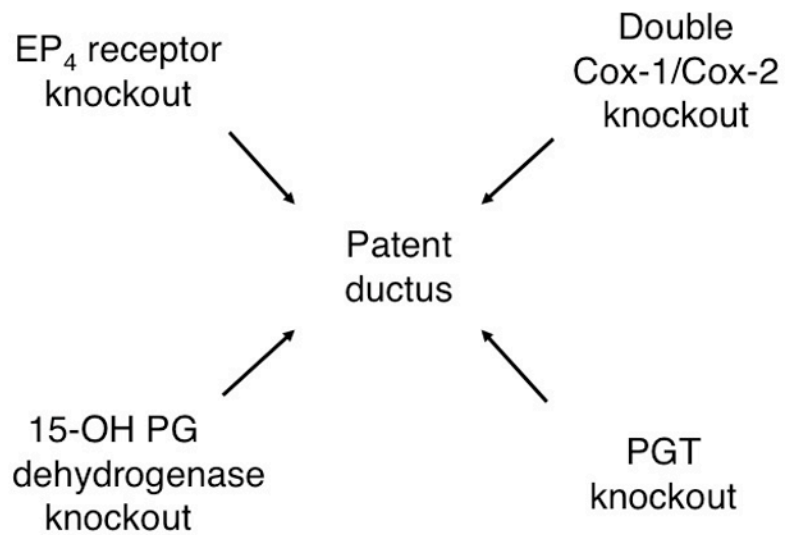


**Figure 7.** Patent ductus arteriosus resulting from perturbations of PGE<sub>2</sub> signaling. Genetic interruption of both COX enzymes, or genetic interruption of the EP<sub>4</sub> receptor, of prostaglandin dehydrogenase (PGDH), or of PGT (present work) all result in PDA in the mouse. Further detail and references are given in the Discussion.